Can Tho University Journal of Science
website: ctujs.ctu.edu.vn

DOI: 10.22144/ctu.jen.2022.039

Structural and electronic properties of hydrogen - functionalized armchair germanene nanoribbons: A first-principles study

Nguyen Duy Khanh[1,2*], Nguyen Thi Hong Hue[3], Nguyen Thanh Tien[3], and Vo Van On[1*]

[1]*Institute of Applied Technology, Thu Dau Mot University, Binh Duong Province, Viet Nam*

[2]*High-Performance Computing Laboratory (HPC Lab), Thu Dau Mot University, Binh Duong Province, Viet Nam*

[3]*College of Natural Sciences, Can Tho University, Can Tho City, Viet Nam*

**Correspondence: Nguyen Duy Khanh (email: khanhnd@tdmu.edu.vn);*
Vo Van On (email: onvv@tdmu.edu.vn)

Article info.

Received 03 Dec 2021
Revised 09 Jan 2022
Accepted 01 Mar 2022

Keywords

Armchair germanene nanoribbons, band structure, charge transfer, DFT calculation, graphene, germanene, and hydrogen functionalization

ABSTRACT

Structural and electronic properties of armchair germanene nanoribbons functionalized by hydrogen atoms (H-AGeNR) are studied through density functional theory (DFT) method. The DFT quantities for analyzing the structural and electronic properties are fully developed through the DFT calculations, including the functionalization energy, relaxed geometric parameters, orbital- and atom-decomposed energy bands, electronic density of states, charge density, and charge density difference. Under hydrogen functionalization, the functionalization energy is achieved at -2.59 eV, and the structural parameters are slightly distorted. This provides evidence of good structural stability of the functionalized system. Besides, the very strong bonds of H-Ge are created because the electrons are transfered from Ge atoms to H adatoms, which induces hole density in the functionalized system, which is regarded as p-type doping. As a result, the π bonds of $4p_z$ orbitals at low-lying energy are fully terminated by the strong H-Ge covalent bonds, in which the strong hybridizations of H-1s and Ge-(4s, $4p_x$, $4p_y$, and $4p_z$) orbitals have occurred at deep valence band. The termination of π bonds leads to the opened energy gap of 2.01 eV in the H-functionalized system that belongs to the p-type semiconductor. The enriched properties of the H-functionalized system identify that the H-functionalized system can be promissing 1D semiconductor for high-performance optoelectronic applications.

1. INTRODUCTION

Since the first two-dimensional (2D) graphene monolayer made of carbon elements arranged in a planar hexagonal lattice was successfully synthesized (Novoselov et al., 2004), it strongly motivated many further studies of graphene-like 2D materials owing to its novel and unique properties to significantly enhance performance for applications as compared with the traditional bulk materials (Acun et al., 2015; Balendhran et al., 2015; Nguyen et al., 2019; Nguyen et al., 2020). As a close analog of graphene, germanene made of germanium (Ge) elements arranged in a low-buckled hexagonal lattice has attracted plenty of efforts because the Ge constituents have good compatibility with the silicon elements in the current semiconducting industry and the low-buckled structure of

germanene also possesses better stability than the planar graphene in devices (Kaloni et al., 2013; Nijamudheen et al., 2015; Zhang et al., 2016). However, the zero-gap feature of 2D germanene is a critical drawback that creates barrier the use of germanene for electronic applications. Thus, opening a bandgap for germanene is an essential issue for practical applications that have recently increased attention in the scientific community (Yao et al., 2018; Qin et al., 2017). Various approaches have been utilized to open bandgap for germanene, including functionalization (Pang et al., 2015), adsorption (Hoat et al., 2021) substitution (He et al., 2021), inducing defects (Monshi et al., 2017), forming stacking configurations (Pang et al., 2011), applying external electric or magnetic fields (Hattori et al., 2019), and creating finite-size confinements (Sharma et al., 2021). Among these methods, the finite-size confinements of the 2D germanene resulting in the one-dimensional (1D) germanene that can enhance bandgap without any serious deformations in geometries are a very effective way to open bandgap for germanene.

This 1D germanene is termed germanene nanoribbons (GeNRs), in which the different edge terminations that can create two typical germanene nanoribbons are armchair (AGeNR) and zigzag (ZGeNR) germanene nanoribbons (Sharma et al., 2017; Shiraz et al., 2019). It should be noted that the bandgaps of GeNRs strongly depend on their widths, and the different edge configurations exhibit different electronic and magnetic behaviors. The direct energy gap comes to exist in the germanene nanoribbons with armchair edge, which belongs to the non-magnetic semiconductor. Meanwhile, the germanene nanoribbons with zigzag edge displays the semiconducting behavior with the anti-ferromagnetic states across the edges, in which each zigzag edge presents opposite ferromagnetic states. Nevertheless, the opened bandgaps of GeNRs are too narrow to have good compatibility with the optoelectronic applications that require bandgaps larger than 0.7 eV (Pang et al., 2011). Thus, enhancing the bandgap of GeNRs is an essential topic for both electronic and optoelectronic applications that have gained popularity in many recent studies. Many methods to enhance bandgap for GeNRs have been studied, including the inducing defects (Samipour et al., 2020a), external fields (Matthes et al., 2014), stacking configurations (Arjmand et al., 2018), atom dopings (Samipour et al., 2020b), and edge or surface functionalizations (Liu et al., 2017; Sharma et al., 2018). Among these methods, the surface functionalization's by hydrogen atoms can significantly enhance the bandgap of GeNR with good structural stability owing to strong H-Ge bonds that is worthy of a detailed investigation. In this study, the structural and electronic properties of H-AGeNR are investigated using the high-performance DFT calculations. Through the high-performance DFT calculations, the DFT quantites for analyzing the geometric structures and electronic bahviors are fully developed such as the functionalization energies, relaxed structural parameters, electronic energy bands, electronic density of states, spatial charge distributions, and charge distribution difference. The developed first-principles DFT quantites can be utilize for many other doped systems.

2. COMPUTATIONAL METHOD

Both the geometric structure and electronic behavior of H-AGeNR were determined by the DFT method, which is performed in Vienna Ab Initio Simulation Package (VASP) (Kresse et al., 1996). The VASP jobs were carried out by the high performance computing cluster at Thu Dau Mot University. The VASP jobs were constituted by four input files, including the POTCAR, KPOINTS, POSCAR, and INCAR, in which the POTCAR file is constructed by the Perdew-Burke-Ernzerhof (PBE) functional for evaluating the electron-electron interaction (Perdew et al., 1996) and the projector-augmented wave (PAW) pseudopotentials for calculating the intrinsic electron-ion interactions. The KPOINTS file for 1D structure is constructed by 1×1×12 k-point meshes for relaxing structure and incresed k-point meshes of 1×1×100 for calculating the elecronic quantites. To create the monolayer, a vacuum space of 20 Å is used in the POSCAR file. In the relax step, tags of NSW=600, EDIFF=1E-6, and EDIFFG=-0.01 are used in the INCAR file to calculate the ionic relaxation, energy convergence, and maximum Hellman-Feynman force, respectively. For calculating the electronic quantites, tag of ICHARG=11 is used in the INCAR for evaluating the charge density and the band line mode along Γ to K is used in the KPOINTS file to calculate the electronic band structure.

3. RESULTS AND DISCUSSION

3.1. Structural properties

Geometric structures of germanene nanoribbon with armchair edge without surface functionalization (pristine AGeNR) and germanene nanoribbons with

armchair edge under hydrogen functionalization (H-AGeNR) are shown in Figs. 1(a) and 1(b), respectively, in which projection in (x,y) plane and (y,z) plane to show for top view and side view is presented in the left and righ hand side in the Fig. 1. The width of germanene nanoribbons is described by dimer line along y direction and width of six dimer lines is used in the study model.

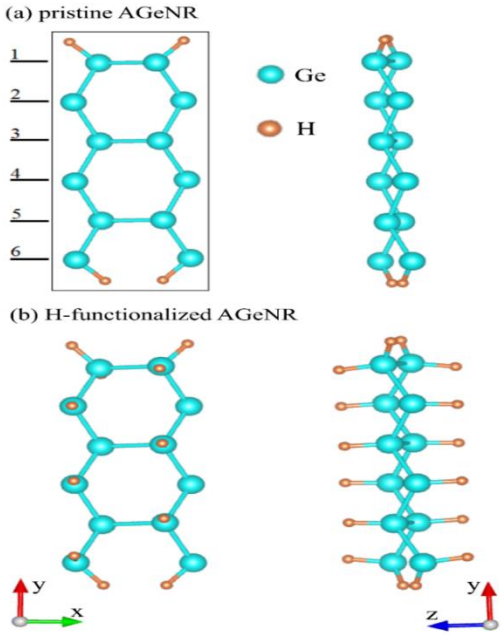

Figure 1. Geometric structure projected in the top view and side view of (a) the pristine AGeNR and (b) H-AgeNR, in which the black lines along y direction are described for the withd of AGeNR

The dangling bonds along armchair edges were removed by attaching to four hydrogen atoms along armchair edges. Under relaxed calculations, the favorable functionalization of hydrogen adatoms were found at the top sites of the system among other sites, and the only double-side functionalization of H-AGeNR can lead to the stable structure that is evaluated by the functionalized energy (E_{func}), while the single-side functionalization generates the unstable structure. The E_{func} is calculated as follows:

$$E_{func} = \left(E_{tot} - E_{pris} - nE_H\right)/n \qquad (1)$$

In the above equation, denotation of E_{tot}, E_{pris}, and E_H are responsible for the energy of the functionalized system, energy of pristine system, and energy of isolated hydrogen adatoms, respectively; denotation of n is shown for the total number of surface hydrogen adatoms. The calculated E_{func} is valued at -2.59 eV as shown in Table 1. This E_{func} value is large enough to form a stable functionalized structure. Under the double-side functionalization effect, H-Ge bond length of 1.55 Å is induced, which is very shorter than Ge-Ge bond length of 2.37 Å as displayed in Table 1. This means that the generated bond of H-Ge is very stronger than the bond of Ge-Ge. Due to the effect of finite-size termination, the bond length of Ge-Ge at the armchair edge (1st Ge-Ge) is larger than the bond length of Ge-Ge at far armchair edge (2nd Ge-Ge), in which the 1st Ge-Ge bond lengths of 2.39 Å and 2.37 Å and the 2nd Ge-Ge bond lengths of 2.36 Å and 2.35 Å correspond to the pristine AGeNR and H-AgeNR as illustrated in Table 1. Also, it can be identified that the Ge-Ge bond lengths of the H-AGeNR are slightly shorter than that of the pristine system. The buckling height of 0.91 Å in the H-AGeNR is shorter than that of 1.08 Å in the pristine AGeNR, confirming that the buckling is reduced under the H functionalization. The shorter bond lengths and buckling result in the larger bond angle of Ge-Ge-Ge of 114.25 (˚) in the hydrogen functionalized system, as compared with the pristine system. This indicates that the H-AGeNR possesses a more symmetric lattice than the pristine AGeNR. The pristine system exhibits the orbital hybridization of mixed sp^2/sp^3 in buckled Ge-Ge bonds, in which the strongly bonded σ network made of the 4s, $4p_x$, and $4p_y$ orbitals and the insignificant π bonds of $4p_z$ orbitals. Such weak π bonds are fully terminated under the H functionalization that creates the hybridization mechanism of $1s\text{-}sp^3$ in H-Ge bonds.

3.2. Electronic properties

The 1D energy bands of the pristine germanene nanoribbons and hydorgen-functionalized germanene nanoribbons is shown in Fig. 2, in which the Fermi level is located at the zero energy to distinguish the bandgap and electronic states illustrated by short dot black lines. The electronic band structure of the pristine armchair germanene nanoribbon in Fig. 2(a) presents a direct energy gap of 0.23 eV as shown in Table 1. There is a asymmetry between the valence and conduction band in the 1D energy bands in Fig. 2(a), which is determined from the Fermi level. The asymmetric 1D subbands are anti-crossing. Different dominations of Ge-orbitals in 1D subbands are identified by the orbital-decomposed band structure. Specifically, Ge-$4p_z$ orbitals illustrated through red circles in Fig. 2(a) significantly dominate at the

long-range energies near the Fermi level from -2.6 eV to 2.6 eV that indicates for long-range π bands, in which the co-domination of $4p_z$ orbitals and ($4p_x$ and $4p_{y)}$ orbitals shown by the blue circles exists at the valence band from -2.6 eV upward the conduction band; the strongest distribution of Ge-$4p_z$ is from the lowest conduction band upward higher energy. From middle valence band of -2.6 eV to deeper range energies, the Ge-($4p_x$+$4p_y$) orbitals are strongly dominated and co-dominated with the Ge-4s orbital shown by the green circles at the deepest range energies, whereas the domination of Ge-$4p_z$ orbitals is disappeared. It should be noted that the co-domination of 4s orbitals and ($4p_x$ and $4p_y$) orbitals imply sp^2 hybridization, while co-domination of 4s orbitals, ($4p_x$ and $4p_y$) orbitals, and $4p_z$ orbitals illustrate for sp^3 hybridization. This can clarify that the hybridization of mixed sp^2/sp^3 is occurred in the pristine system, which is responsible for the co-dominated band of σ and π orbitals.

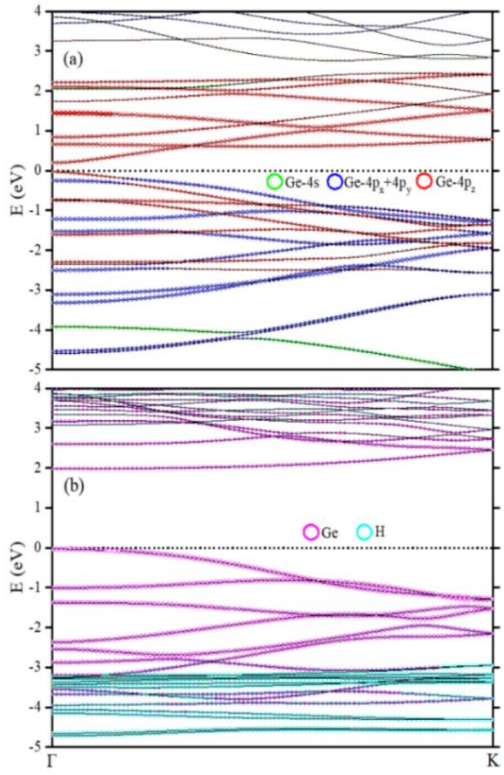

Figure 2. Orbital- and atom-dominated energy band of (a) pristine AGeNR and (b) H-AGeNR

Under the hydrogen functionalization, the 1D energy band of the pristine system is dramatically changed, as shown in Fig. 2(a), whereas the bandgap is much enlarged at 2.01 eV. the cyan circles. This is due to the that the bond length of H-Ge is very shorter than the bond length of Ge-Ge. The Ge atoms fully dominate at long-range energies from -3.2 eV to 4 eV illustrated by pink circles in Fig. 2(a), which determine the opened bandgap, while the hydrogen atoms strongly dominate at deep valence energies from -3.2 eV to -5 eV.

The orbital-decomposed density of states (DOSs) was utilized to affirm the electronic energy band. The DOSs of the pristine system and H-functionalized systems are shown in Figs. 3(a) and 3(b), respectively, in which the Fermi energy is illustrated by the black short dot lines. The DOSs of the pristine system in Fig. 3(a) shows a vacant region in vicinity of Fermi level, which evidences for the energy gap. The peaks of $4p_z$ orbitals illustrated by red curves at long-range energies near the Fermi level are resulted from the low-lying π bands, whereas the $4p_z$ peaks are stronger than the peaks made of 4s orbitals illustrated by green curves and ($4p_x$ and $4p_y$) orbitals illustrated by blue curves above the Fermi level, while the $4p_x$ and $4p_y$ orbitals-made peaks are stronger distributed than the $3p_z$ peaks below the Fermi level; however, the 4s, Ge-$4p_z$, ($4p_x$ and $4p_y$) peaks simultaneously appear in long-range π regions. This confirms the sp^3 hybridization. Below the middle valence energy of -2.6 eV, the $3p_z$ peaks are almost disappeared, and there only exist the merged 4s, ($4p_x$ and $4p_y$) peaks, whereas ($4p_x$ and $4p_y$) peaks is more dominant than the 4s peak, indicating for the sp^2 hybridization. In the whole energy range, it can show that the mixed sp^2/sp^3 hybridization is appeared. Under the H functionalization, the DOSs was fully reshaped as shown in Fig. 3(b). The appearance of bonds of H-Ge creates significant peaks at the deep valence range merged with the 1s orbitals and 4s orbitals, ($4p_x$+$4p_y$) orbitals, and $4p_z$ orbitals, in which the 1s peaks are stronger than the other peaks. This illustrates the hybridization of 1s-sp^3 in H-Ge bonds. The π peaks at long-range energies in Fig. 3(a) are disappeared because of the destroy of π bonds in Fig. 3(b), whereas the 4s orbitals- and ($4p_x$ and $4p_y$) orbitals-made peaks fully dominate at long-range energies.

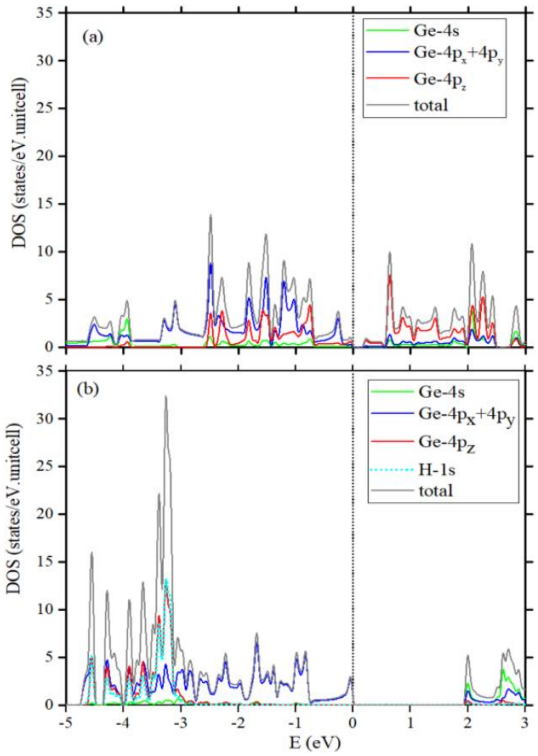

Figure 3. Orbital-decomposed DOSs of (a) pristine AGeNR and (b) H-AGeNR

The bonding magnitude and hybridization mechanism are verified through the charge density distribution. The charge density distribution of the pristine system and hydrogen-functionalized system is shown in Figs. 4(a) and 4(b), respectively. The highest and lowest charge densities were used to display for strongest and weakest bonds, as illustrated by the red and blue colors, respectively. The charge density of the pristine system illustrated in Fig. 4(a) shows a strong charge distribution between two Ge atoms as displayed by the red region, which is owing to the strong σ bonds of Ge-Ge. Meanwhile, the charge distribution is quite lower in the z-direction displayed by the green region between two Ge atoms that is owing to the weak π Ge-Ge bonds. From the clear information on the charge density, it can be mentioned that the bond of σ is very stronger than the bond of π, and strong bonds of σ form the stable monolayer structure. The H-AGeNR functionalization causes much change in the charge density illustrated in Fig. 4(b), whereas the weak bond of π is destroyed by forming in very strong covalent bonds of H-Ge, and H-Ge bonds (dark red region) are stronger than the bonds of Ge-Ge because the bond length of H-Ge is very shorter than the bond length of Ge-Ge as identified in Table 1, while the σ Ge-Ge bond in the H-AGeNR are enhanced as compared with the pristine σ bonds owing to the Ge-Ge bond lengths shortened under the H-functionalization as identified in Table 1. To observe mechanism of charge transfer, the charge density difference of the H-AGeNR is presented in Fig. 4(c), whereas the red and blue regions are responsible for vanished and gained electrons, respectively. This shows that the electrons are transfer from Ge atoms to H adatoms. This charge transfer process creates the hole density in the H-AGeNR, which is regarded as the p-type system.

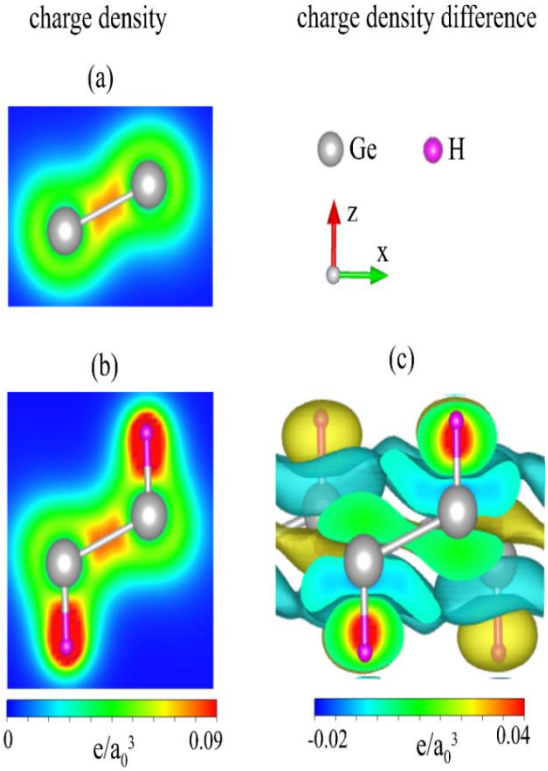

Figure 4. Charge density distributions of (a) pristine system and (b) H-functionalized system; and charge density difference distribution of (c) H-AGeNR

Table 1. E_{func}(eV), Ge-Ge bond lengths, bond length of H-Ge (Å), buckling height (Å), bond angle of Ge-Ge-Ge (˚), and energy gap [E_g (eV)] of the pristine system and H-functionalized system at the with of six dimer lines

Configurations	E_{func} (eV)	1st Ge-Ge (Å)	2nd Ge-Ge (Å)	H-Ge (Å)	Ge-Ge-Ge angle (˚)	Buckling (Å)	E_g (eV)
pristine system	X	2.396	2.362	X	107.74	1.087	0.23
H-system	-2.59360	2.378	2.355	1.55	114.25	0.919	2.01

4. CONCLUSION

The geometric structure and electronic behavior of the pristine AGeNR and H-AGeNR were fully revealed in the physical quantities developed under the DFT calculations, including the functionalization energies, relaxed geometric parameters, electronic energy bands, electronic density of states (DOSs), charge density, and charge density difference. The calculated functionalization energies demonstrate that the H functionalization can create a stable 1D structure. The created bond of H- Ge is very stronger than the bonds of Ge-Ge that fully terminate the π bonds and slightly distort the σ bonds. The formation of strong H-Ge bonds is due to the transfer of electrons from Ge atoms to H adatoms that create the 1s-sp^3 hybridization mechanism.

As a close relationship, the significant change in geometric structure in the H-AGeNR results in their enriched electronic properties. The bandgap of 2.01 eV is opened in the H-AGeNR, and this bandgap is determined by the σ orbitals of Ge atoms. The enriched properties under the H functionalization effect offer great potential for optoelectronic applications that require a bandgap larger than 0.7 eV.

ACKNOWLEDGMENTS

This research is funded by Thu Dau Mot University, Binh Duong Province, Vietnam under grant number DA.21.1-003, and this research used resources of the high-performance computer cluster (HPCC) at Thu Dau Mot University

REFERENCES

Acun, A., Zhang, L., Bampoulis, P., Farmanbar, M. V., van Houselt, A., Rudenko, A. N & Zandvliet, H. J. (2015). Germanene: the germanium analog of graphene. *Journal of Physics: Condensed Matter*, 27(44), 443002.

https://doi.org/10.1088/0953-8984/27/44/443002

Arjmand, T., Tagani, M. B., & Soleimani, H. R. (2018). Buckling-dependent switching behaviours in shifted bilayer germanene nanoribbons: A computational study. *Superlattices and Microstructures*, 113, 657-666.

https://doi.org/10.1016/j.spmi.2017.11.052

Balendhran, S., Walia, S., Nili, H., Sriram, S., & Bhaskaran, M. (2015). Elemental analogues of graphene: silicene, germanene, stanene, and phosphorene. *Small*, 11(6), 640-652.

https://doi.org/10.1002/smll.201402041

Hattori, A., Yada, K., Araidai, M., Sato, M., Shiraishi, K., & Tanaka, Y. (2019). Influence of edge magnetization and electric fields on zigzag silicene, germanene and stanene nanoribbons. *Journal of Physics: Condensed Matter*, 31(10), 105302.

https://doi.org/10.1088/1361-648X/aaf8ce

He, J., Liu, G., Wei, L., & Li, X. (2021). Effect of Al doping on the electronic structure and optical properties of germanene. *Molecular Physics*, e2008540.

https://doi.org/10.1080/00268976.2021.2008540

Hoat, D. M., Nguyen, D. K., Ponce-Pérez, R., Guerrero-Sanchez, J., Van On, V., Rivas-Silva, J. F., & Cocoletzi, G. H. (2021). Opening the germanene monolayer band gap using halogen atoms: An efficient approach studied by first-principles calculations. *Applied Surface Science*, 551, 149318.

https://doi.org/10.1016/j.apsusc.2021.149318

Kaloni, T. P., & Schwingenschlögl, U. (2013). Stability of germanene under tensile strain. *Chemical Physics Letters*, 583, 137-140.

https://doi.org/10.1016/j.cplett.2013.08.001

Kresse, G., & Furthmüller, J. (1996). Efficient iterative schemes for ab initio total-energy calculations using a plane-wave basis set. *Physical Review B*, 54(16), 11169.

https://doi.org/10.1103/PhysRevB.54.11169

Liu, J., Yu, G., Shen, X., Zhang, H., Li, H., Huang, X., & Chen, W. (2017). The structures, stabilities, electronic and magnetic properties of fully and partially hydrogenated germanene nanoribbons: A first-principles investigation. *Physica E: Low-dimensional Systems and Nanostructures*, 87, 27-36.

https://doi.org/10.1016/j.physe.2016.11.018

Matthes, L., & Bechstedt, F. (2014). Influence of edge and field effects on topological states of germanene

nanoribbons from self-consistent calculations. *Physical Review B*, 90(16), 165431.
https://doi.org/10.1103/PhysRevB.90.165431

Monshi, M. M., Aghaei, S. M., & Calizo, I. (2017). Doping and defect-induced germanene: A superior media for sensing H_2S, SO_2, and CO_2 gas molecules. *Surface Science*, 665, 96-102.
https://doi.org/10.1016/j.susc.2017.08.012

Novoselov, K. S., Geim, A. K., Morozov, S. V., Jiang, D. E., Zhang, Y., Dubonos, S. V & Firsov, A. A. (2004). Electric field effect in atomically thin carbon films. *Science*, 306(5696), 666-669.
https://www.science.org/doi/10.1126/science.1102896

Nguyen, D. K., Tran, N. T. T., Chiu, Y. H., Gumbs, G., & Lin, M. F. (2020). Rich essential properties of Si-doped graphene. *Scientific Reports*, 10(1), 1-16.
https://doi.org/10.1038/s41598-020-68765-x

Nguyen, D. K., Tran, N. T. T., Chiu, Y. H., & Lin, M. F. (2019). Concentration-diversified magnetic and electronic properties of halogen-adsorbed silicene. *Scientific Reports*, 9(1), 1-15.
https://doi.org/10.1038/s41598-019-50233-w

Nijamudheen, A., Bhattacharjee, R., Choudhury, S., & Datta, A. (2015). Electronic and chemical properties of germanene: the crucial role of buckling. *The Journal of Physical Chemistry C*, 119(7), 3802-3809.
https://doi.org/10.1021/jp511488m

Pang, Q., Li, L., Zhang, L. L., Zhang, C. L., & Song, Y. L. (2015). Functionalization of germanene by metal atoms adsorption: a first-principles study. *Canadian Journal of Physics*, 93(11), 1310-1318.
https://doi.org/10.1139/cjp-2015-0206

Pang, Q., Zhang, Y., Zhang, J. M., Ji, V., & Xu, K. W. (2011). Electronic and magnetic properties of pristine and chemically functionalized germanene nanoribbons. *Nanoscale*, 3(10), 4330-4338.
https://doi.org/10.1039/C1NR10594A

Perdew, J. P., Burke, K., & Ernzerhof, M. (1996). Generalized gradient approximation made simple. *Physical Review Letters*, 77(18), 3865.
https://doi.org/10.1103/PhysRevLett.77.3865

Qin, Z., Pan, J., Lu, S., Shao, Y., Wang, Y., Du, S., & Cao, G. (2017). Direct evidence of Dirac signature in bilayer germanene islands on Cu (111). *Advanced Materials*, 29(13), 1606046.
https://doi.org/10.1002/adma.201606046

Samipour, A., Dideban, D., & Heidari, H. (2020a). Impact of an antidote vacancy on the electronic and transport properties of germanene nanoribbons: A first principles study. *Journal of Physics and Chemistry of Solids*, 138, 109289.
https://doi.org/10.1016/j.jpcs.2019.109289

Samipour, A., Dideban, D., & Heidari, H. (2020b). Impact of substitutional metallic dopants on the physical and electronic properties of germanene nanoribbons: A first principles study. *Results in Physics*, 18, 103333.
https://doi.org/10.1016/j.rinp.2020.103333

Sharma, V., & Srivastava, P. (2021). Silicene and Germanene Nanoribbons for Interconnect Applications. In Nanoelectronic Devices for Hardware and Software Security (pp. 85-100). *CRC Press*.
https://doi.org/10.1201/9781003126645

Sharma, V., Srivastava, P., & Jaiswal, N. K. (2018). Edge-oxidized germanene nanoribbons for nanoscale metal interconnect applications. *IEEE Transactions on Electron Devices*, 65(9), 3893-3900.
https://doi.org/10.1109/TED.2018.2858006

Sharma, V., Srivastava, P., & Jaiswal, N. K. (2017). Prospects of asymmetrically H-terminated zigzag germanene nanoribbons for spintronic application. *Applied Surface Science*, 396, 1352-1359.
https://doi.org/10.1016/j.apsusc.2016.11.161

Shiraz, A. K., Goharrizi, A. Y., & Hamidi, S. M. (2019). The electronic and optical properties of armchair germanene nanoribbons. *Physica E: Low-dimensional Systems and Nanostructures*, 107, 150-153.
https://doi.org/10.1016/j.physe.2018.11.019

Yao, Q., Zhang, L., Kabanov, N. S., Rudenko, A. N., Arjmand, T., Rahimpour Soleimani, H., & Zandvliet, H. J. W. (2018). Bandgap opening in hydrogenated germanene. *Applied Physics Letters*, 112(17), 171607.
https://doi.org/10.1063/1.5026745

Zhang, L., Bampoulis, P., Rudenko, A. N., Yao, Q. V., Van Houselt, A., Poelsema, B., & Zandvliet, H. J. W. (2016). Structural and electronic properties of germanene on MoS_2. *Physical Review Letters*, 116(25), 256804.
https://doi.org/10.1103/PhysRevLett.116.256804